Demonstration of laser pulse amplification by stimulated Brillouin scattering

E. Guillaume, K. Humphrey, H. Nakamura, R. M. G. M. Trines, R. Heathcote, M. Galimberti, Y. Amano, D. Doria, G. Hicks, E. Higson, S. Kar, G. Sarri, M. Skramic, J. Swain, K. Tang, J. Weston, P. Zak, E. P. Alves, R. A. Fonseca, F. Fiúza, H. Habara, K. A. Tanaka, R. Bingham, M. Borghesi, Z. Najmudin, L. O. Silva and P. A. Norreys

High Power Laser Science and Engineering / Volume 2 / September 2014 / e33
DOI: 10.1017/hpl.2014.35, Published online: 25 September 2014

Link to this article: http://journals.cambridge.org/abstract_S2095471914000358

How to cite this article:
E. Guillaume, K. Humphrey, H. Nakamura, R. M. G. M. Trines, R. Heathcote, M. Galimberti, Y. Amano, D. Doria, G. Hicks, E. Higson, S. Kar, G. Sarri, M. Skramic, J. Swain, K. Tang, J. Weston, P. Zak, E. P. Alves, R. A. Fonseca, F. Fiúza, H. Habara, K. A. Tanaka, R. Bingham, M. Borghesi, Z. Najmudin, L. O. Silva and P. A. Norreys (2014). Demonstration of laser pulse amplification by stimulated Brillouin scattering. High Power Laser Science and Engineering, 2, e33 doi:10.1017/hpl.2014.35

High Power Laser Science and Engineering, (2014), Vol. 2, e33, 6 pages.

doi:10.1017/hpl.2014.35

Demonstration of laser pulse amplification by stimulated Brillouin scattering

E. Guillaume[1,2], K. Humphrey[3], H. Nakamura[4], R. M. G. M. Trines[2], R. Heathcote[2], M. Galimberti[2], Y. Amano[5], D. Doria[6], G. Hicks[4], E. Higson[7], S. Kar[6], G. Sarri[6], M. Skramic[8], J. Swain[7], K. Tang[7], J. Weston[7], P. Zak[7], E. P. Alves[9], R. A. Fonseca[9], F. Fiúza[9], H. Habara[5], K. A. Tanaka[5], R. Bingham[2,3], M. Borghesi[6], Z. Najmudin[4], L. O. Silva[9], and P. A. Norreys[7,2]

[1]*Laboratoire d'Optique Appliquée, Ecole Polytechnique, Palaiseau, 91128, France*

[2]*STFC Rutherford Appleton Laboratory, Didcot, Oxon OX11 0QX, United Kingdom*

[3]*University of Strathclyde, Glasgow G1 1XQ, United Kingdom*

[4]*Blackett Laboratory, Imperial College London, Prince Consort Road, London SW7 2BZ, United Kingdom*

[5]*Graduate School of Engineering, Osaka University, Japan*

[6]*Queens University Belfast, Belfast BT7 1NN, United Kingdom*

[7]*University of Oxford, Parks Road, Oxford OX1 3PU, United Kingdom*

[8]*University of Cambridge, Cambridge CB2 1TQ, United Kingdom*

[9]*GoLP/Instituto de Plasmas e Fusão Nuclear - Laboratorio Associado, Instituto Superior Técnico, 1049-001 Lisbon, Portugal*

(Received 23 May 2014; revised 1 August 2014; accepted 6 August 2014)

Abstract

The energy transfer by stimulated Brillouin backscatter from a long pump pulse (15 ps) to a short seed pulse (1 ps) has been investigated in a proof-of-principle demonstration experiment. The two pulses were both amplified in different beamlines of a Nd:glass laser system, had a central wavelength of 1054 nm and a spectral bandwidth of 2 nm, and crossed each other in an underdense plasma in a counter-propagating geometry, off-set by 10°. It is shown that the energy transfer and the wavelength of the generated Brillouin peak depend on the plasma density, the intensity of the laser pulses, and the competition between two-plasmon decay and stimulated Raman scatter instabilities. The highest obtained energy transfer from pump to probe pulse is 2.5%, at a plasma density of $0.17n_{cr}$, and this energy transfer increases significantly with plasma density. Therefore, our results suggest that much higher efficiencies can be obtained when higher densities (above $0.25n_{cr}$) are used.

Keywords: laser–plasma interactions; optical pulse generation and compression; stimulated Brillouin and Raman scattering; ultra-fast optical processes

1. Introduction

Exploration of the intensity frontier is an exciting challenge for physicists. Advances in laser technologies, particularly those associated with increased power and decreased pulse duration, are of great interest due to their application to many fields in science and engineering, for example in laser-driven inertial fusion energy, in laser- and beam-driven particle accelerators, and in next-generation light sources. Currently, most high power lasers rely on the chirped pulse amplification (CPA) technique, in which a laser pulse is stretched before going to an amplifying medium, then expanded to large area (1 m or more) and recompressed, in order to avoid optical damage that occurs at intensities close to 10^{12} W cm^{-2}. Present-day high power lasers typically reach around 1 PW peak powers. Next-generation laser systems have been designed to reach powers of 10 PW or more, by the employment of the optical parametric CPA (OPCPA) technique. However, the achievement of intensities beyond this level is still uncertain, mainly due to the requirement for precise wavefront delivery at the final focusing optic of multiple large area laser beams.

Pulse compression methods using plasmas have been promoted as a way of overcoming these obstacles. The enormous energy densities associated with focused high power

Correspondence to: P. A. Norreys, Clarendon Laboratory, University of Oxford (& STFC Rutherford Appleton Laboratory), Parks Road, Oxford OX1 3PU, UK.

lasers excite nonlinear wave amplification in a medium that is already ionized. The plasma can support intensities of up to 10^{17} W cm^{-2}, i.e., 5 orders of magnitude larger than solid-state systems, before disruption to the medium occurs[1]. Laser pulse amplification in plasma rests upon an energy transfer between a relatively long duration pump pulse and a shorter seed pulse through the generation of either an electron plasma wave, known as stimulated Raman scattering (SRS), or an ion-acoustic wave, known as stimulated Brillouin scattering (SBS). Experimental[2] and numerical[3, 4] results have already been demonstrated in the case corresponding to SRS excitation.

As SBS produces a frequency shift in the scattered wave spectra, it is necessary for the seed laser to be downshifted by an amount equal to the ion-acoustic frequency in order for coupling between the laser beams to be realized. When utilizing long duration beams, which naturally have a very narrow bandwidth, an adjustment to the seed laser is essential for coupling between the laser beams to ensure that the necessary frequency component for scattering is present in the seed. This creates an additional technical complexity to the achievement of Brillouin scattering in plasma. However, when the seed beam is sufficiently short, and its bandwidth is sufficiently wide, the necessary downshifted frequency to trigger Brillouin scattering of the pump pulse will already be available in the seed pulse, and no additional frequency modification will be needed.

In this paper, we report on experimental observations of Brillouin scattering using two beams incident from the same laser system, one long (15 ps) pump beam and one short (1 ps) seed beam counter-propagating with respect to one another through a volume of plasma, with no modifications made to the frequency of either pulse. These findings are corroborated by 1D numerical simulations using the particle-in-cell code OSIRIS[5], confirming that for sufficiently short pulses the necessary Brillouin downshifted frequency is presented in the laser bandwidth, therefore negating the requirement for a frequency downshift in the seed pulse to be performed before Brillouin scattering can be obtained. A pump-to-probe energy transfer of up to 2.5% has been obtained, which confirms earlier results by Lancia *et al.*[6], who obtained 2.25% in a similar experiment.

In addition, our results extend the results by Lancia *et al.*[6] in two important ways. First, we found that the energy transfer efficiency increases consistently with density for $0.017 < n_e/n_{cr} < 0.17$. This may indicate that our plasma density showed fewer spatial fluctuations, which were suspected to reduce the efficiency in the earlier experiment. Second, we found in our numerical simulations that there is significant competition between SRS and SBS. This both reduces the efficiency and indicates that much better results may be obtained for $n_e > 0.25 n_{cr}$, where Raman scattering is no longer possible. These new results reveal how Brillouin amplification depends on the experimental parameters, and show how future experiments should be set up for enhanced performance.

2. Theory

SBS in plasmas can be characterized as the scattering of a high frequency transverse electromagnetic wave by a low frequency ion-acoustic wave into a second transverse electromagnetic wave. This corresponds to the decay of an incident photon in the laser beam, with frequency ω_0 and wavenumber k_0, into a phonon (ion-acoustic quantum) with frequency ω_{IAW} and wavenumber k_{IAW}, and a scattered photon, with frequency ω_s and wavenumber k_s, which travels in approximately the opposite direction to the incoming laser photon. Following directly from linear theory[7], the frequency and wavenumber matching conditions, often invoked when studying the Brillouin instability, are

$$\omega_0 = \omega_s + \omega_{\mathrm{IAW}}, \tag{1}$$

$$k_0 = k_s + k_{\mathrm{IAW}}, \tag{2}$$

where ω_{IAW} and k_{IAW} are the frequency and wavenumber of the ion-acoustic wave, respectively. The maximum growth occurs when (for pure backscattering)

$$k_{\mathrm{IAW}} = 2k_0 - \frac{2\omega_0}{c}\frac{c_s}{c}, \tag{3}$$

$$\gamma = \frac{1}{2\sqrt{2}}\frac{ck_0 a_0 \omega_{pi}}{\sqrt{\omega_0 k_0 c_s}}. \tag{4}$$

Here, $\sqrt{\omega_0^2 - \omega_{pe}^2}$ is the wavenumber of the pump laser wave in plasma, ω_0 and ω_{pe} are the laser and electron plasma frequencies, respectively, $c_s = \sqrt{T_e/m_i}$ is the ion sound speed, T_e is the electron temperature, m_i is the ion mass and $\omega_{pi} = \omega_{pe}\sqrt{m_e/m_i}$ is the ion plasma frequency.

In the case of Raman amplification, the minimum frequency shift that can occur is equal to the plasma frequency, meaning that the maximum density where Raman amplification techniques can be utilized is one quarter of the critical density. However, in the case of Brillouin amplification, the minimum frequency shift is equal to zero, therefore allowing Brillouin scattering to operate at densities up to the critical density[8]. In addition to this, more energy can be transferred into the scattered wave via Brillouin scattering than via Raman scattering as less energy is coupled into the ion-acoustic wave in Brillouin scattering than the Langmuir wave associated with Raman scattering. This makes the Brillouin mechanism particularly useful for applications such as laser amplification techniques[6, 9] and induced energy transfer between adjacent laser beams at facilities such as the National Ignition Facility[10, 11].

3. Experimental setup

The experiment was conducted on the Vulcan Nd:glass laser facility at the Rutherford Appleton Laboratory[12]. This

facility provided two linearly polarized laser pulses of $\lambda_0 = 1054$ nm central wavelength with a $\Delta\lambda_0 = 2$ nm bandwidth. The two laser beam diameters were reduced to 20 mm using pierced plastic plates, in order to have the correct spot size on the target. Each laser pulse was focused onto the target using $f/30$ off-axis parabolic mirrors, with $f = 612$ mm focal length, giving focal spots of 130 µm diameter. The pump beam contained between 570 and 860 mJ of energy, with a pulse duration $\tau_{\text{pump}} = 15$ ps, giving a pump intensity on the target of around 3×10^{14} W cm^{-2}. The seed beam contained between 38 and 477 mJ, with a pulse duration $\tau_{\text{seed}} = 1$ ps, giving a seed intensity on the target of between 2.5×10^{14} and 3.3×10^{15} W cm^{-2}. The laser pulses were injected into the target from opposite directions, with an angle of 10° between the two counter-propagating beams. This angle was used for safety reasons; while it led to a small reduction in pulse growth, this was deemed acceptable. A 1.65 mm long overlap distance was achieved in this geometrical setup. The temporal delay between the pump and the seed was adjusted so that the two ascending edges of the pulses crossed in the center of the gas target in order to maximize the duration of the interaction. This was achieved by using a streak camera looking at the overlap region. The laser pulses were focused in the center of a 5 mm long supersonic gas jet target, using either argon or deuterium. The gas target produced uniform plasmas when ionized, with background electron densities n_e varying between 1.7×10^{17} and 1.7×10^{20} cm^{-3}. The plasma density was controlled by adjusting the backing pressure of the supersonic gas jet. The plasma is created by the interaction pulses themselves – without any ionization pulse needed – triggering multiphoton ionization of the gas and collisions between electrons and atoms.

The light transmitted through the plasma in the direction of propagation of the seed beam was collected and collimated using a 600 mm focal length lens. The collimated beam was then steered out of the target chamber using flat silver mirrors, and focused onto the entrance slit of an optical spectrometer, equipped with a 150 lines/mm diffraction grating coupled with an Andor 16-bit CCD camera recording the spectra with a 0.1 nm resolution. A schematic diagram of the experiment can be seen in Figure 1. It should be noted that the transmitted seed was measured only for the case of the seed and the pump interacting with parallel horizontal polarizations.

4. Experimental results

The results of the experiment are shown in Figure 2. Figure 2 shows three optical spectra of the transmitted laser light taken at different plasma densities, with different laser configurations. Figure 2(a) represents the transmitted spectrum passing through the gas jet, with the pump beam turned off. Figures 2(b) and (c) show the transmitted spectra through the gas jet in the presence of the pump beam, for two

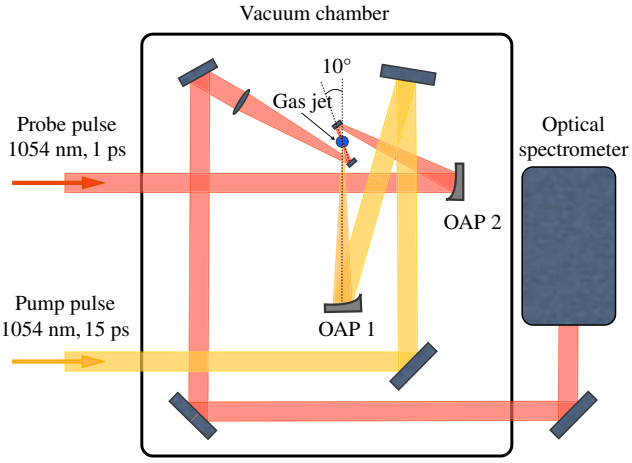

Figure 1. Schematic diagram of the experimental setup.

different plasma densities (1.7×10^{19} and 1.7×10^{20} cm^{-3}, respectively). The interaction with the gas jet and the pump beam clearly modifies the transmission spectrum of the seed. In the shot without a pump beam (Figure 2(a)), the propagation of the seed pulse through the plasma causes the formation of a small secondary peak, at $\omega/\omega_0 = 0.9975$. Since the separation between the peaks is much smaller than the plasma frequency for this configuration, the peak cannot correspond to SRS, and is presumed to correspond to spontaneous SBS by the seed pulse. The addition of an energetic pump beam, while keeping the plasma density the same, significantly enhances this downshifted spectral peak, proving that we have obtained pump-to-seed energy transfer via stimulated Brillouin backscattering. By increasing the plasma density by an order of magnitude, one can observe a significant increase of the relative intensity and energy content of the peaks: the secondary peak is now only 3.5 times smaller than the fundamental. It should be noted that for experimental shots with similar laser parameters, but with plasma densities between 1.7×10^{17} and 1.8×10^{18} cm^{-3}, no secondary peaks could be observed.

The energy transfer efficiency is calculated as follows. For the laser shot depicted in Figure 2(c), the pump energy was 675 mJ after passage through the 20 mm diameter aperture, while the seed pulse energy was 86 mJ. From the vacuum shot and the height of the Brillouin peak in Figure 2(c), it can be deduced that the Brillouin peak contains about 20% of the original seed energy, or 17 mJ. This corresponds to a 2.5% energy transfer efficiency from pump to seed.

5. Numerical simulations

The numerical simulations were conducted in 1D using the fully relativistic particle-in-cell (PIC) code OSIRIS[5] and were constructed to mirror the experimental parameters as closely as possible. For these simulations, the plasma

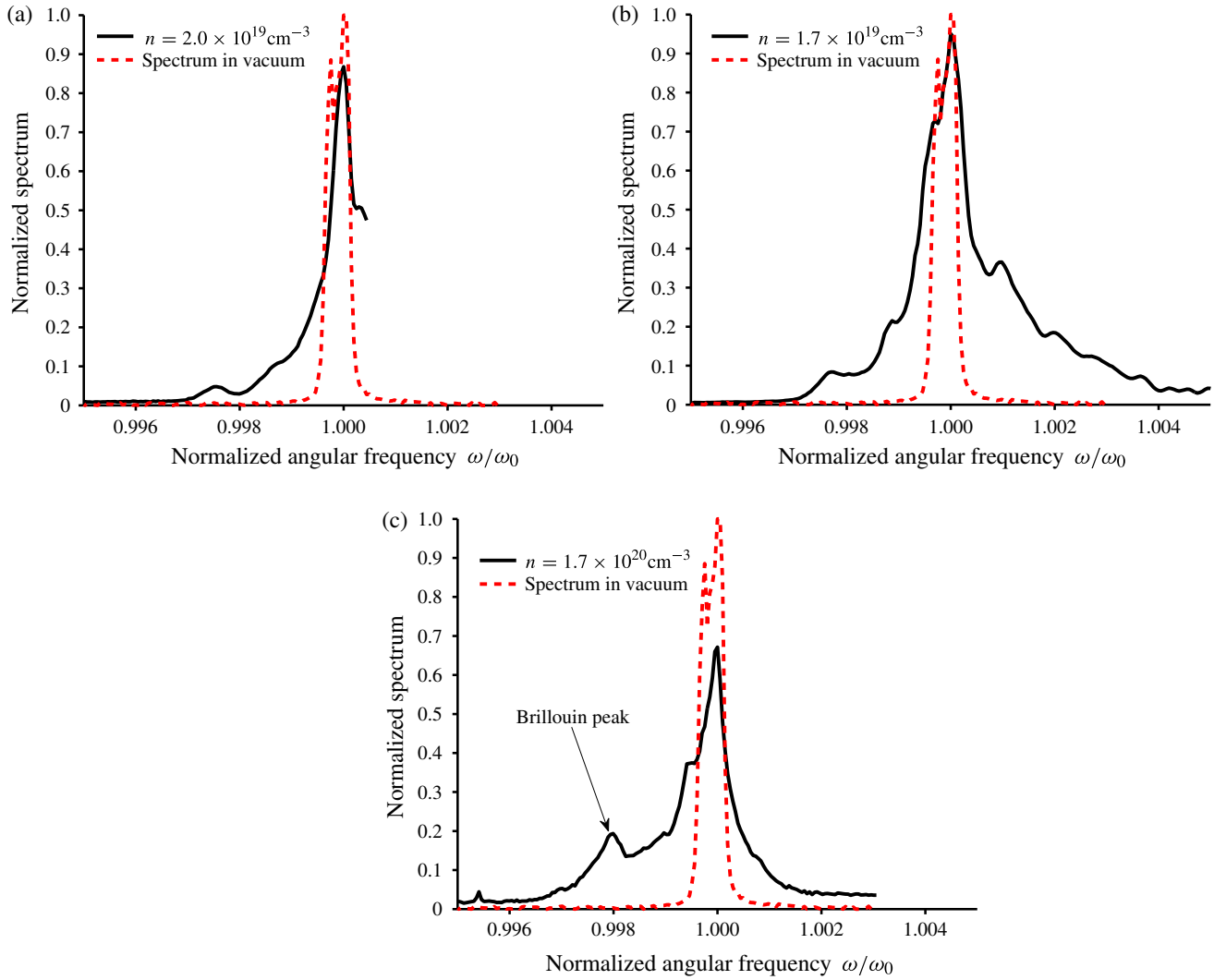

Figure 2. Experimental frequency spectra of a 1 ps laser pulse recorded after propagation through a supersonic gas jet (normalized intensity versus normalized angular frequency). A reference spectrum, recorded with the gas jet turned off, has been included in each plot. Graph (a) is the spectrum recorded with only the seed beam at an intensity of 4.0×10^{14} W cm^{-2} interacting with the gas jet at $n_e = 2.0 \times 10^{19}$ cm^{-3}, without a counter-propagating pump beam. Graph (b) was recorded with the two counter-propagating beams interacting, the seed at an intensity of 3.6×10^{15} W cm^{-2} and the pump at 4.2×10^{14} W cm^{-2}, at $n_e = 1.7 \times 10^{19}$ cm^{-3}. Graph (c) was recorded with the seed at an intensity of 3.2×10^{14} W cm^{-2} and the pump at 3.2×10^{14} W cm^{-2}, at $n_e = 1.7 \times 10^{20}$ cm^{-3}. The generation of a downshifted peak can be observed through the interaction of the laser pulses and the gas jet, with its relative intensity compared to the fundamental peak strongly depending on the plasma density and the presence of a counter-propagating pump pulse.

electron temperature and the effective ionization degree of the atoms are needed. These quantities were calculated using the laser plasma simulation code MEDUSA, in 1D planar geometry, using a corrected Thomas–Fermi equation-of-state model and an average-atom model, and assuming collisional ionization. For the shots shown in Figure 2, this yields $T_e = 130$, 120, and 5 eV, respectively, and $Z^* = 5.5$, 1.0, and 1.1. These values were used to estimate the plasma electron density for each case, which was used in the OSIRIS simulations.

Three sets of simulation results corresponding to each of the three experimental regimes examined are presented, and were set up as follows. In simulation (a) a single laser of intensity 6×10^{14} W cm^{-2} was injected into an argon plasma of density $0.018 n_c$ with a mass ratio of ions to electrons of $m_i/m_e = 14{,}688$. The plasma temperature ratio was set such that $ZT_e/T_i = 25$, where $Z = 5$ and $T_e = 20$ eV, assuming neon-like argon with the majority of the outer shell of electrons depleted. For simulation (b) two counter-propagating pulses were launched into a plasma of density $0.015 \times n_c$, in this case comprising deuterium, with a mass ratio of ions to electrons of $m_i/m_e = 3672$, with the plasma ion and electron temperatures kept constant at 20 eV for the ions and 120 eV for the electron species. Laser intensities of 6.2×10^{14} and 5.4×10^{14} W cm^{-2} for the pump and seed, respectively, were used, where the seed pulse was launched at the instant the pump laser had traversed the length of the plasma. In the case of simulation (c), two counter-

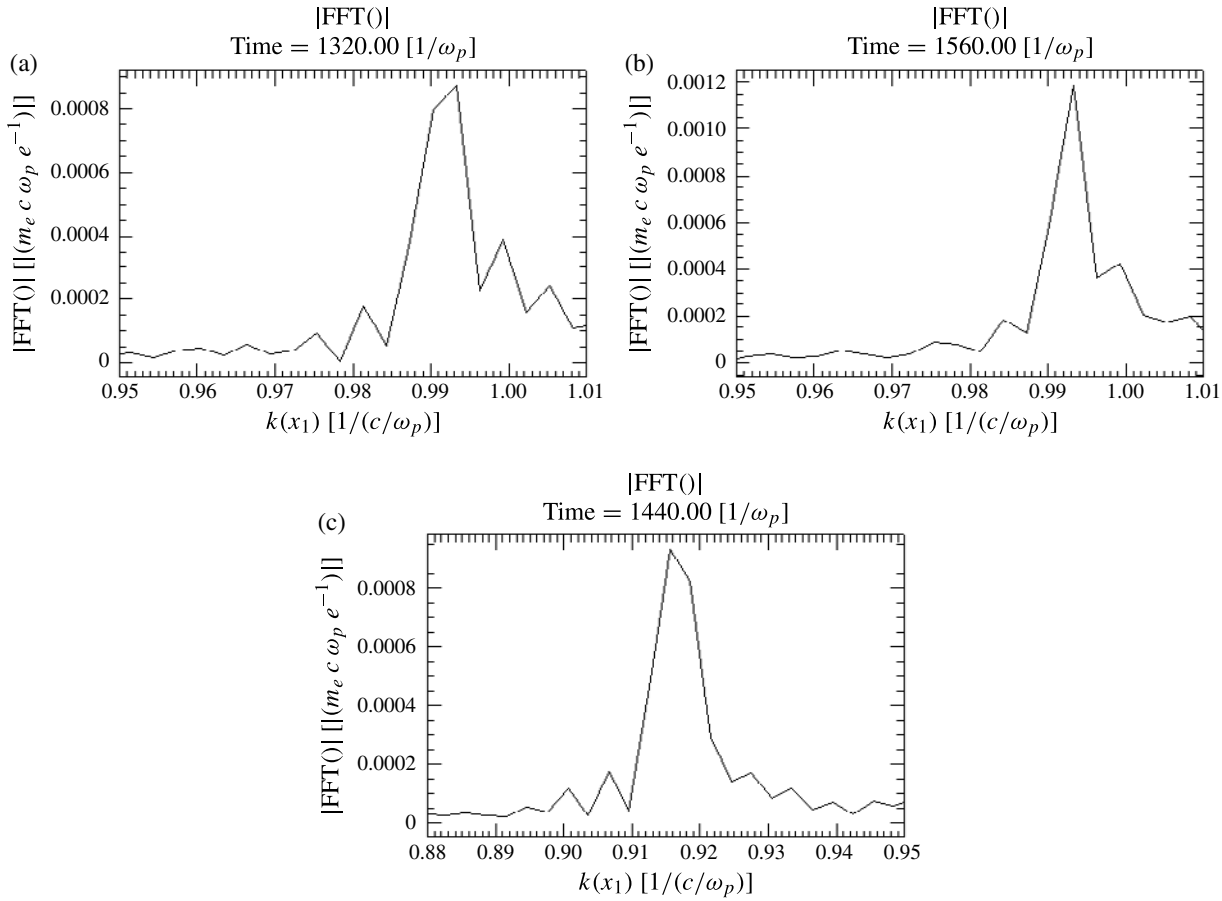

Figure 3. Simulated spectra corresponding to each of the experimental regimes presented in Figure 2 (normalized intensity versus normalized wavevector). The electron density varied from 1.7×10^{19} to 1.7×10^{20} cm^{-3}. Graph (a) is the spectrum simulated with a single laser of intensity 6×10^{14} W cm^{-2} interacting in a neon-like argon plasma with an electron temperature of about 20 eV and density of $0.018n_c$. Graph (b) was calculated with the two counter-propagating beams interacting in a deuterium plasma of density $0.015 \times n_c$, the seed at intensity 5.4×10^{15} W cm^{-2} and the pump at 6.2×10^{14} W cm^{-2}, with an electron temperature of 120 eV. Graph (c) was simulated with the seed at intensity 4.9×10^{14} W cm^{-2} and the pump at 4.9×10^{14} W cm^{-2}, in an argon plasma with an electron temperature of 5 eV and a density of $0.16n_c$.

propagating beams were used and their intensities were both set to 4.9×10^{14} W cm^{-2} and propagated through an argon plasma with a configuration such that $m_i/m_e = 73{,}440$, $ZT_e/T_i = 5$, where $Z = 1$ and $T_e = 5$ eV, and a density of $0.16n_c$. The following parameters are consistent throughout each of the three simulations presented: the pulses propagate through a plasma column of length $1410c/\omega_0$, with the pump pulse traveling from right to left through the simulation box; the pump pulse has a duration of 1.5 ps and the seed pulse a duration of 100 fs; each of the pulses is from a laser of wavelength 1 μm; the time step for integration is $\Delta t = 0.04\omega_p^{-1}$, where ω_p is the plasma electron frequency; the spatial resolution of the simulations is of the order of the Debye length, with 100 particles per cell. Due to computational limitations, the pulse lengths and plasma column were scaled down by a factor of ten from the parameters used to obtain the experimental results.

Upon examination of the spectra presented in Figure 3, it can be seen that the results obtained by OSIRIS closely match the results obtained from the experimental observations of Brillouin scattering shown in Figure 2. In each of the three cases examined numerically, however, it can be seen that the Fourier spectrum obtained is slightly broader than that of the experimental results. This slight variation in the spectra is attributed to the fact that the simulations have no transverse dimensions as they were performed in 1D, hence putting numerical constraints on the solutions obtained as there can be no transverse variation of the laser intensity. Therefore, the amplitude of any plasma wave driven by the laser will be overestimated, which leads to an overestimation of spectral drifts and also of the temperature recorded.

6. Conclusions

These experimental observations of Brillouin scattering using two beams at the same wavelength are a promising confirmation of the observations by Lancia *et al.*[6] that

energy transfer by SBS can be achieved with a single laser system, with no frequency downshift required in the seed pulse, as is mandatory to perform Raman amplification. In addition, we have revealed that an increase in the plasma density leads to an increase in the energy transfer efficiency, because of the increased Brillouin growth rate and the disappearance of Raman scattering above $0.25n_{cr}$. The generation of a Brillouin peak using the natural bandwidth of the laser is confirmed by the 1D PIC simulation results from OSIRIS. The same PIC simulations also revealed significant competition between SRS and SBS, for densities between $0.017n_{cr}$ and $0.17n_{cr}$. The experiments revealed a substantial increase in the SBS signal with increasing plasma density, in line with the theoretically predicted increase of the growth rate. In light of these results, it is recommended that future Brillouin amplification experiments are carried out at plasma densities above $0.25n_{cr}$ to eliminate SRS altogether and benefit from the higher Brillouin scattering growth rate.

Acknowledgements

The authors would like to gratefully acknowledge the support of the staff of the Central Laser Facility for their help. They would also like to thank R. Kirkwood, S. Wilks, D. Meyerhofer, S. Craxton, D. Froula, J. Myatt and A. Solodov for useful discussions. This work was supported by the UK Science and Technology Facilities Council and by the Engineering and Physical Sciences Research Council. H.N. was supported by the Royal Society Newton International Fellowship and the Japan Society for the Promotion of Science.

References

1. N. J. Fisch and V. M. Malkin, Phys. Plasmas **10**, 2056 (2003).
2. J. Ren, S. Li, A. Morozov, S. Suckewer, N. A. Yampolsky, V. M. Malkin, and N. J. Fisch, Phys. Plasmas **15**, 056702 (2008).
3. R. M. G. M. Trines, F. Fiúza, R. Bingham, R. A. Fonseca, L. O. Silva, R. A. Cairns, and P. A. Norreys, Nature Phys. **7**, 87 (2010).
4. R. M. G. M. Trines, F. Fiúza, R. Bingham, R. A. Fonseca, L. O. Silva, R. A. Cairns, and P. A. Norreys, Phys. Rev. Lett. **107**, 105002 (2011).
5. R. A. Fonseca, L. O. Silva, F. S. Tsung, V. K. Decyk, W. Lu, C. Ren, W. B. Mori, S. Deng, S. Lee, T. Katsouleas, and J. C. Adam, Lect. Notes Comput. Sci. **2331**, 342 (2002).
6. L. Lancia, J.-R. Marquès, M. Nakatsutsumi, C. Riconda, S. Weber, S. Hüller, A. Mančić, P. Antici, V. T. Tikhonchuk, A. Héron, P. Audebert, and J. Fuchs, Phys. Rev. Lett. **104**, 025001 (2010).
7. D. W. Forslund, J. M. Kindel, and E. L. Lindman, Phys. Fluids **18**, 1002 (1975).
8. W. L. Kruer, *The Physics of Laser Plasma Interactions* (Westview Press, 2003).
9. A. A. Andreev, C. Riconda, V. T. Tikhonchuk, and S. Weber, Phys. Plasmas **13**, 053110 (2006).
10. P. Michel, L. Divol, E. A. Williams, C. A. Thomas, D. A. Callahan, S. Weber, S. W. Haan, J. D. Salmonson, N. B. Meezan, O. L. Landen, S. Dixit, D. E. Hinkel, M. J. Edwards, B. J. MacGowan, J. D. Lindl, S. H. Glenzer, and L. J. Suter, Phys. Plasmas **16**, 042702 (2009).
11. P. Michel, S. H. Glenzer, L. Divol, D. K. Bradley, D. Callahan, S. Dixit, S. Glenn, D. Hinkel, R. K. Kirkwood, J. L. Kline, W. L. Kruer, G. A. Kyrala, S. Le Pape, N. B. Meezan, R. Town, K. Widmann, E. A. Williams, B. J. MacGowan, J. Lindl, and L. J. Suter, Phys. Plasmas **17**, 056305 (2010).
12. C. N. Danson, P. A. Brummitt, R. J. Clarke, J. L. Collier, B. Fell, A. J. Frackiewicz, S. Hancock, S. Hawkes, C. Hernandez-Gomez, P. Holligan, M. H. R. Hutchinson, A. Kidd, W. J. Lester, I. O. Musgrave, D. Neely, D. R. Neville, P. A. Norreys, D. A. Pepler, C. J. Reason, W. Shaikh, T. B. Winstone, R. W. W. Wyatt, and B. E. Wyborn, Nucl. Fusion **44**, S239 (2004).